AIMS Bioengineering, 9(2): 178–196.
DOI: 10.3934/bioeng.2022013
Received: 28 March 2022
Revised: 22 May 2022
Accepted: 25 May 2022
Published: 30 May 2022

http://www.aimspress.com/journal/Bioengineering

Research article

Fast delivery of melatonin from electrospun blend polyvinyl alcohol and polyethylene oxide (PVA/PEO) fibers

Rachel Emerine and Shih-Feng Chou*

Department of Mechanical Engineering, College of Engineering, The University of Texas at Tyler, Tyler TX, 75799, USA

* **Correspondence:** Email: schou@uttyler.edu; Tel: +19035666209.

Abstract: Water-soluble polymers possess great advantages in current drug delivery systems, such as fast delivery through polymer matrix dissolution as well as promoting solid dispersion of poorly water-soluble drugs. In this work, water-soluble polyvinyl alcohol (PVA) and polyethylene oxide (PEO) were blended (50/50) to electrospin with and without the incorporation of a model drug, melatonin (MLT), at various blend polymer concentrations. Results suggested that increasing blend PVA/PEO solution concentrations, up to 7 wt%, promoted the formation of smooth and defect-free drug-incorporating fibers with an average fiber diameter ranged from 300 to 700 nm. Mechanical properties of the blank and MLT-loaded PVA/PEO fibers showed dependence on fiber morphologies and fiber mat structures, due to polymer concentrations for electrospinning. Furthermore, the surface wettability of the blend PVA/PEO fibers were investigated and further correlated with the MLT release profile of the fibers. Results suggested that fiber mats with a more well-defined fiber structure promoted a linear release behavior within 10 minutes in vitro. These drug-incorporated fibers were compatible to human umbilical vein endothelial cells (HUVECs) up to 24 hours. In general, this work demonstrated the structure-property correlations of electrospun PVA/PEO fibers and their potential biomedical applications in fast delivery of small molecule drugs.

Keywords: water-soluble polymers; electrospun fibers; mechanical properties; fast/burst release; cell compatibilities

1. Introduction

Topical drug delivery via mucosal membranes often requires the use of water-soluble polymers due to their excellent mucosal adhesiveness. Upon absorption of physiological fluids, polymer matrix swelling and molecular chain disentanglements facilitate the diffusion and dissolution of the small molecule drugs through mucosal membranes. In addition, water-soluble polymers are particularly useful carriers in drug delivery systems (DDS) for fast drug delivery applications of poorly water-soluble small molecule drugs that have a short half-life time and/or with a poor solid dispersion [1,2]. For example, drug-polymer conjugates, block copolymers, hydrogels, and other drug-polymer complexes using synthetic and natural water-soluble polymers have been reviewed in the context of drug delivery in pharmaceutical applications [3].

Among all current commercially available water-soluble polymers, polyvinyl alcohol (PVA) and polyethylene oxide (PEO) have attracted much attention in fast drug delivery due to their excellent biocompatibility [4]. Combined with their fast water dissolution rates, blend PVA/PEO polymers have shown advantages as a polymer matrix for mucosal drug delivery in the form of oral strips [5]. In addition, due to the semi-crystalline molecular structures of both polymers, polymeric drug carriers using PVA/PEO are able to provide some levels of mechanical strength and flexibility for user applications. Therefore, PVA/PEO blend-based nano- and micro-particles, fibers, films, hydrogels, and freeze-dried scaffolds, were developed to enable controlled release of small molecule drugs (seconds to hours) by mechanisms of polymer matrix dissolution, osmosis, ion-exchange, and drug diffusion [6].

Electrospinning is a fiber producing technique that utilizes charged electrons, applied through an external electric field, to move polymer liquid over a distance to a deposition collector plate [7]. During the travelling of the polymer liquid, solvent evaporates through a "whipping" process and continuous solid fibers are produced with average fiber diameters ranging from several hundred nanometers to a few micrometers [8]. The resulting fiber mats are able to exhibit a nonwoven and/or an aligned fiber structure, depending on the types of the collector used. Nonetheless, electrospun drug-containing fibers provide a high surface area to volume ratio, suitable for diffusion- and dissolution-determined drug delivery processes. In addition, electrospun microfibers are capable of encapsulating a large amount of drug (up to 40%) while being able to provide sustained, multi-staged, or fast drug delivery characteristics [9–11].

Melatonin, *N*-acetyl-5-methoxytryptamine ($C_{13}H_{16}N_2O_2$), is a natural endocrine hormone produced by pineal gland, which regulates sleep and other biological activities in human. Melatonin is a small molecule (M_w = 232 g/mol) with amphiphilic nature (LogP = 1.42) allowing it to quickly pass through the lipid bilayer of the cell membranes. Melatonin has been widely used to treat sleep disorders through oral delivery, and it is required to reach a maximum concentration at around 50 minutes making fast release of melatonin from solid dosages a necessity. A recent study described the uses of melatonin-loaded mesoporous silica nanoparticles coated with cellulose acetate phthalate for fast release in oral drug delivery, and the results showed a three-stage release mechanism up to 75% of cumulative release after 2 hours [12]. Recent studies showed that melatonin exhibited free radical scavenging activities, and it had strong docking ability with the three proteins, 6LU7, 6M03, and 6W63, on COVID-19 virus, suggesting melatonin as an medical adjuvant to treat COVID-19 patients [13].

In this work, we explore the use of blend PVA/PEO polymers through the electrospinning process to encapsulate a model drug, melatonin (MLT), for fast drug delivery applications. In particular, we investigated the effects of solution properties on electrospun blank and MLT-loaded PVA/PEO fibers. Fiber morphology and average fiber diameter studies showed the dependence on blend PVA/PEO concentrations. In addition, the mechanical properties of the blend PVA/PEO fibers corresponded to the fiber morphologies and fiber mat structures. More importantly, we investigated the dissolution properties of the electrospun blend PVA/PEO fibers. Our data suggested the fast release of MLT from PVA/PEO fibers with a rate dependence on the blend fiber concentrations. Furthermore, cytotoxicity studies suggested that both blank and MLT-loaded PVA/PEO fibers were compatible to endothelial cells up to 24 hours. In general, our current study correlated the processing-structure-property relationships of MLT-loaded electrospun blend PVA/PEO fibers with indications on fast drug delivery for topical and/or mucosal applications.

2. Materials and methods

2.1. Materials

Polyethylene oxide (PEO) with an average molecular weight (M_w) of 900 kDa was obtained from DuPont (Midland, MI USA). Polyvinyl alcohol (PVA), Elvanol® 71-30 (fully hydrolyzed, viscosity of 27 ~ 33 cP using 4 wt% at 20 °C), was kindly supplied from Kuraray America Inc. (Houston, TX USA). The viscosity data of the PVA (#341584, M_w 89,000 – 98,000, and 99+% hydrolyzed) from Sigma-Aldrich was 11.6 – 15.4 cP using 4 wt% at 20 °C, indicating that the M_w of the Elvanol® 71-30 was higher than that of the Sigma-Aldrich. Melatonin (MLT), 99% pure with an average molecular weight (M_w) of 232.28 g/mol, was purchased from BeanTown Chemical (Hudson, NH USA). Phosphate-buffered saline (PBS) buffer solution (pH ~ 7.4) was purchased from VWR (Radnor, PA, USA). All the other chemicals were of reagent grade and used as received without further purification.

2.2. Preparation of polymer solutions

Various concentrations of PVA/PEO blend solutions were prepared by dissolving pre-measured amounts of PVA and PEO powders in deionized water (DI-water) using glass vials. Briefly, the total mass of polymer powder was measured to achieve polymer concentrations of 5, 6, and 7 wt% (w/v). The volumetric blend ratio (v/v) of PVA and PEO was 50/50 for the three polymer concentrations. These polymer solutions were then placed in a water bath on a stirring hot plate for mixing at 80 °C using magnetic stir bars. After complete mixing of the PVA/PEO (50/50) blend solutions at various polymer concentrations, pre-determined amounts of melatonin powders were added to the polymer solutions at 5% w/w loading (drug/overall solids) followed by continuous mixing for an hour. Each solution was visually examined before characterization and electrospinning.

2.3. Solution properties measurements

Solution viscosities were measured using a US Solid rotary viscometer (USS-DVT4) (Cleveland, OH, USA). The viscometer was first balanced and stabilized, and rotor #4 was used for

the measurements (10^4 ~ 10^5 mPa.s). The rotor was then slowly brought down into the polymer solutions until it reached the mark on the rotor for viscosity testing. The viscosities at various rotor speeds were measured for each polymer solution.

The initial viscosity measurements were performed at room temperature (~ 20 °C). For viscosity measurements at various temperatures (i.e., 30 °C, 40 °C, and 50 °C), vials of polymer solutions were conditioned in a warm water bath for at least 30 minutes prior to viscosity measurements. Then, the same setup as described above was used to determine the viscosity of the polymer solutions. Results were averaged on three independent measurements (n = 3).

2.4. Electrospinning of PVA/PEO/MLT fibers

The blank and MLT-loaded PVA/PEO fibers were electrospun within 48 hours of the solution preparation. Prior to electrospinning, polymer solution was drawn into a 3 mL Luer-Lok™ BD syringe (Franklin Lakes, NJ, USA) that was attached to a 21 gauge blunt needle. The syringe and needle assembly were then placed onto a NE-1000 programmable single syringe pump (Farmingdale, NY, USA) to deliver polymer solution. During electrospinning, the applied voltages, flowrates of the polymer solution, and the distances from the tip of the needle to the grounded stationary collector for each sample were listed in Table 1. A total of 2 mL of the polymer solution was electrospun from all polymer solutions, and fiber meshes were covered with aluminum foils and stored in a vacuum desiccator prior to characterizations.

Table 1. Electrospinning parameters for blank and MLT-loaded PVA/PEO microfibers.

	Distance (cm)	Voltage (kV)	Electric field strength (kV/cm)	Flow-rate (μL/min)
Blank PVA/PEO Fibers (wt%)				
5%	13	10	0.770	20
6%	13	10	0.770	20
7%	13	10	0.770	20
MLT-loaded PVA/PEO Fibers (wt%)				
5%	13	10	0.770	30
6%	13	10	0.770	20
7%	13	10	0.770	25

2.5. Fiber morphologies and fiber diameter measurements

The morphologies of electrospun blank and MLT-loaded PVA/PEO fibers were evaluated by a Hitachi TM4000Plus (Tokyo, Japan) scanning electron microscope (SEM). Circular disc punches obtained from the fiber mesh were placed on carbon tape. SEM micrographs were acquired at 15 kV, using a spot size 3, and a working distance of 5.5 mm.

Fiber diameters were measured using ImageJ software (National Institutes of Health, Bethesda, MD, USA) on the collected SEM images. 50 random measurements were taken from different fibers in the SEM images to determine the average fibers diameter and the corresponding standard deviations of each sample (n = 50).

2.6. *Mechanical tests*

Uniaxial tensile tests were performed on a single column screw-driven Instron® 3342 universal materials testing machine (Norwood, MA, USA) described in our previous work [14]. Briefly, dog-bone tensile specimens of 22 mm in nominal length and 5 mm in width were prepared by punching the electrospun fiber mats using an ODC stainless steel die (Waterloo ON, Canada) according to ASTM standard D1708-18 [15]. The thickness of each sample at the nominal region was measured by a digital thickness gauge (resolution = 10 μm). The tensile samples were clamped to the tester, equipped with a 100 N load cell, under 24 ± 1 °C and 45 ± 5% RH in accordance with ASTM standard D5034-21 [16]. The applied strain rate was 0.01/s on the samples. Load and displacement data was recorded from the instrument for calculation of the stress-strain curve of each sample. Average values for Young's modulus (slope of the initial linear region), tensile strength (zero slope or the highest stress), and elongation to failure (fracture strain) were determined from five independent samples, each consisting of a stress-strain curve (n = 5).

2.7. Fiber wettability studies

Fiber wettability studies were performed using the sessile drop method followed by an image processing technique to obtain results in average mass losses (e.g. fiber dissolution) and average water contact angles [17]. Briefly, 7/16" diameter circular disks (A_0) were taken from the blank and MLT-loaded PVA/PEO fiber mats using a metal die. Prior to the test, the initial weight (W_i) and thickness (t_i) of fiber discs were measured by a Metter Toledo AG245 analytical balance (Columbus, OH, USA) and a digital thickness gauge (resolution = 10 μm) to determine the apparent density of the fiber mesh according to Equation (1).

$$\rho \ (\mathrm{mg/mm^3}) = \frac{W_\mathrm{i}}{A_0 t_\mathrm{i}} \tag{1}$$

In the dissolution assay, the disc samples were placed on a metal substrate for depositing of a 4-μL water droplet at the center of the fiber mesh. The droplet dissolved the polymer fibers leaving a hole in the middle of the fiber disc and the progress was recorded by a digital camera vertically from the top of the fiber disc for image processing. After 5 seconds, dissolution of the fiber was stabilized and the dissolved area (A_f) was measured using ImageJ software (National Institutes of Health, Bethesda, MD, USA). The dissolved mass (W_d) and the percentage mass loss were calculated using Equation (2) and Equation (3), respectively. Results were averaged on three independent measurements (n = 3).

$$W_\mathrm{d} \ (\mathrm{mg}) = \rho(A_\mathrm{f} t_\mathrm{i}) \tag{2}$$

$$\mathrm{Mass\ Loss}\ (\%) = \left(\frac{W_\mathrm{d}}{W_\mathrm{i}}\right) \times 100\% \tag{3}$$

In the contact angle study, another camera was placed in front of the fiber disc sample to record the initial contact angle, which was defined as the angle between the substrate and the tangent of the droplet upon initial contact, of blank and MLT-loaded PVA/PEO fibers at various polymer concentrations. Picture frames from the recorded videos were withdrawn for software analysis of the

average contact angles using ImageJ software, National Institutes of Health (Bethesda, MD, USA). Results were averaged on three independent measurements (n = 3).

2.8. In vitro drug release studies

7/16" diameter circular disks were taken from each electrospun MLT-loaded PVA/PEO fiber mesh using a metal die. Masses of the disc samples were measured by a Metter Toledo AG245 (Columbus, OH, USA) analytical balance to determine the theoretical MLT loading for each disc sample. 5-mL of PBS (pH ~ 7.3) release media were prepared for each glass vial followed by placing them in a Thermo Scientific^{TM} MaxQ 4450 (Waltham, MA, USA) incubator shaker pre-warmed to 37 °C. MLT-loaded fiber samples were then placed in the vials in the incubator shaker for in vitro sink release of MLT. At predetermined times, a 40-μL sample of the release media, containing unknown concentration of the MLT, was removed from the corresponding vial and placed in a 1.5-mL microcentrifuge tube.

Standard MLT solutions were prepared using serial dilation methods with concentrations of 400, 200, 100, 50, and 25 μg/mL. Liquid specimens of the standard and unknown MLT samples collected at various time points were analyzed using a Thermo Scientific NanoDrop^{TM} 1000 UV-Vis spectrophotometer (Waltham, MA, USA) at 223 and 278 nm [18]. The resulting intensities of MLT from the unknown samples were compared to the standard MLT curves to determine the drug concentrations of the collected liquid samples at each time point to determine the in vitro MLT release rates. Results were averaged on three independent measurements (n = 3).

2.9. In vitro HUVECs viability assays

Human umbilical vein endothelial cells (HUVECs) were obtained from the American Type Culture Collection (ATCC) (Manassas, VA, USA). The cell culture media for this cell line included vascular cell basal medium (ATCC) with endothelial cell growth kit-BBE (ATCC) supplemented with 10% fetal bovine serum (FBS) and 1% antibiotic mixture. HUVEC cultures were incubated in a humidified chamber with 5% CO_2 at 37 ºC followed by sub-culturing the cells in 24-well tissue culture plates with 10,000/well density until reaching 80% confluency prior to cell viability assays.

The HUVECs viability assays were carried out according to a method reported previously [19]. Briefly, control groups were supplemented with treatment carriers of the culture media for 24 hours at 37 ºC. In addition, the experimental groups were subjected to treatment of placing 7/16" diameter fiber discs of the blank and MLT-loaded PVA/PEO fibers electrospun at various concentrations in culture wells followed by the same culture procedures as the control groups. After 24 hours, a 10-μL MTT reagent was added to each well of the culture followed by incubating the culture for 4 hours in the dark in a CO_2 incubator at 37 °C. After the incubation of the cells with the MTT reagent, a 100-μL warm detergent solution was then added to each well to lyse the cells and solubilize the colored crystals for collection of the supernatants. The supernatants were then transferred to a 96-well plate for optical measurements using a Beckman Coulter AD340 plate reader (Brea, CA, USA) at 570 nm absorbance. All experiments were performed in triplicate (n = 3), and the results were expressed as relative cell viability ratio compared to the control groups.

2.10. Statistical analyses

Results were expressed as average ± standard deviation (SD). Statistical studies of the averages were performed using GraphPad Prism (San Diego, CA, USA) on one-way analysis of variance (ANOVA). Significance was accepted with $P < 0.05$.

3. Results and discussion

3.1. Solution properties

The average viscosities of the blank and MLT-loaded PVA/PEO solutions were measured using a rotary viscometer at various rotational speeds (i.e., shear strain rates) and temperatures, and the results are shown in Figure 1. The average viscosities increased when increasing PVA/PEO solution concentrations from 5 to 7 wt% due to the enhanced frictions between the molecular chains in the solution as a result of the applied shear strain rates. Studies suggested that the viscosities of polymer solutions typically ranged from 0.1 – 2 Pa.s for electrospinning [20]. Our findings showed that the average viscosities for both blank and MLT-loaded blend PVA/PEO solution at 5% and 6% polymer concentrations were in agreement with the reported literature values for electrospinning, while the average viscosities of the 7% groups for both blank and MLT-loaded PVA/PEO solutions were slightly higher than the suggested values.

In addition to the dependence of average viscosities on the polymer concentrations, all samples displayed decreases in average viscosities as the shear strain rates increased, suggesting the shear-thinning behavior of the polymer solutions. At the molecular level, shear-thinning behavior of the polymer solutions is considered as an effect of disentanglement of molecular chains of polymers during flow [21]. Others reported a similar shear-thinning behavior from PEO/alginate solutions suitable for electrospinning [22]. The disentanglement effects of the molecular chains were also observed as temperature increased, where all samples showed lowered average viscosities at a higher temperature. The disruptions of hydrogen bonds and intermolecular interactions were more pronounced with the increased in thermal energy to a polymer system resulting in the reduction of polymer solution viscosity [23].

Finally, the blank PVA/PEO solutions at various polymer concentrations exhibited higher average viscosities than those of the MLT-loaded counterparts, suggesting minimal drug-polymer interactions. Specifically, PEO contains ethylene linkages connecting to oxygen atoms as the backbone, which is unable to produce dipole-dipole interactions with MLT. In contrast, PVA has hydroxyl groups capable of forming intermolecular interactions with small molecule drugs. However, MLT has limited molecular interaction sites due to a net charge balance between the carbonyl groups and the neighboring amino groups [24]. Therefore, the addition of the MLT in PVA/PEO had minimal effects in promoting the average viscosities of polymer solutions.

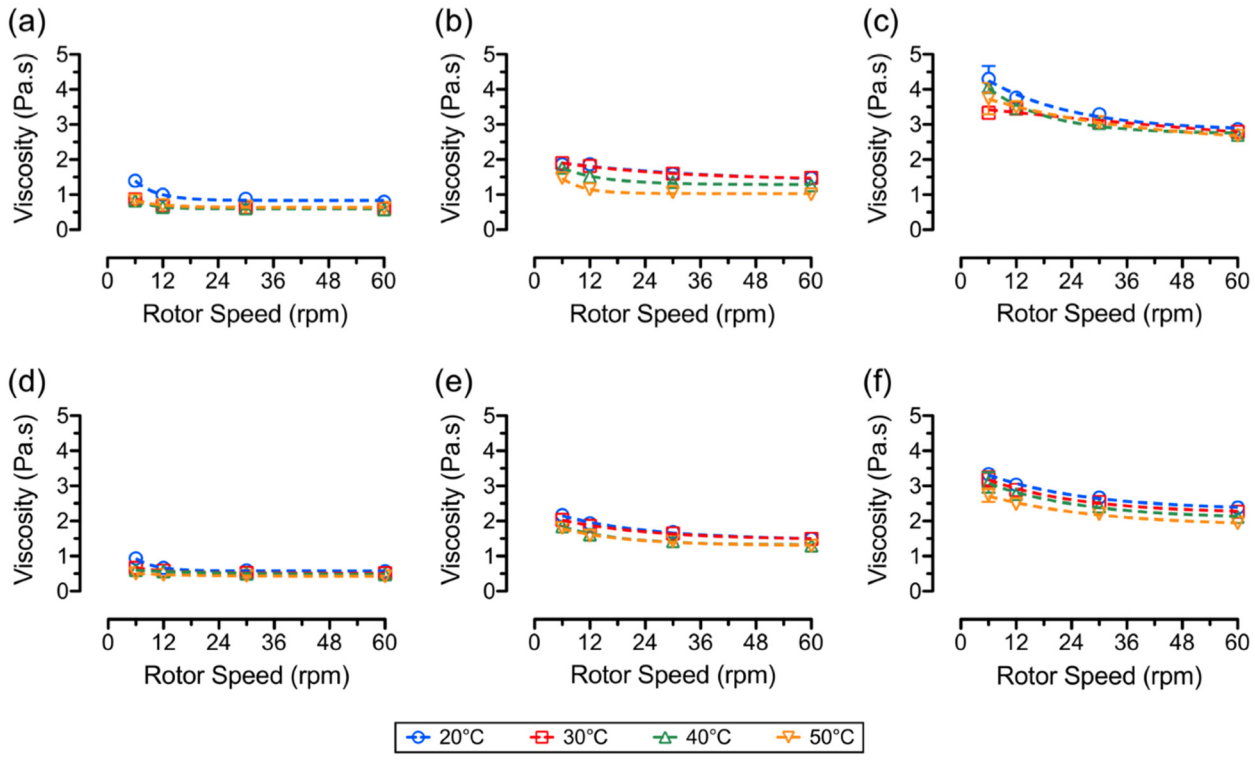

Figure 1. Average viscosities of the blank and MLT-loaded PVA/PEO solutions on the dependence of rotor speeds (i.e., shear strain rates) and temperatures, showing (a) 5 wt%, (b) 6 wt%, and (c) 7 wt% blank PVA/PEO solutions and (d) 5 wt%, (e) 6 wt%, and (f) 7 wt% MLT-loaded PVA/PEO solutions.

3.2. Fiber morphologies and diameters

The fiber morphologies of electrospun blank and MLT-loaded PVA/PEO fibers are shown in Figures 2. In the blank fiber groups, ultrafine fibers with a nonwoven fiber mesh structure were observed with a more well-defined and homogeneous fiber morphologies for the 7 wt% PVA/PEO fibers, whereas the 5 wt% and 6 wt% PVA/PEO fibers exhibited beadings and clumps due to the instability during electrospinning. Similar phenomena of beadings in electrospun fibers were reported when the viscosities of the solutions were low [25]. In contrast, the MLT-loaded PVA/PEO fibers showed spraying and particles forming for the 5 wt% and 6 wt% groups, suggesting the effects of MLT in decreasing the electrospinnability of the PVA/PEO fibers. This observation was in agreement with the low average solution viscosities of the MLT-loaded PVA/PEO groups, suggesting the insufficient chain entanglement in electrospinning. These defects in electrospun MLT-loaded PVA/PEO fibers were minimized after increasing the PVA/PEO solution concentration to 7 wt%, where smooth, defect-free, and drug-incorporated fibers were produced after electrospinning.

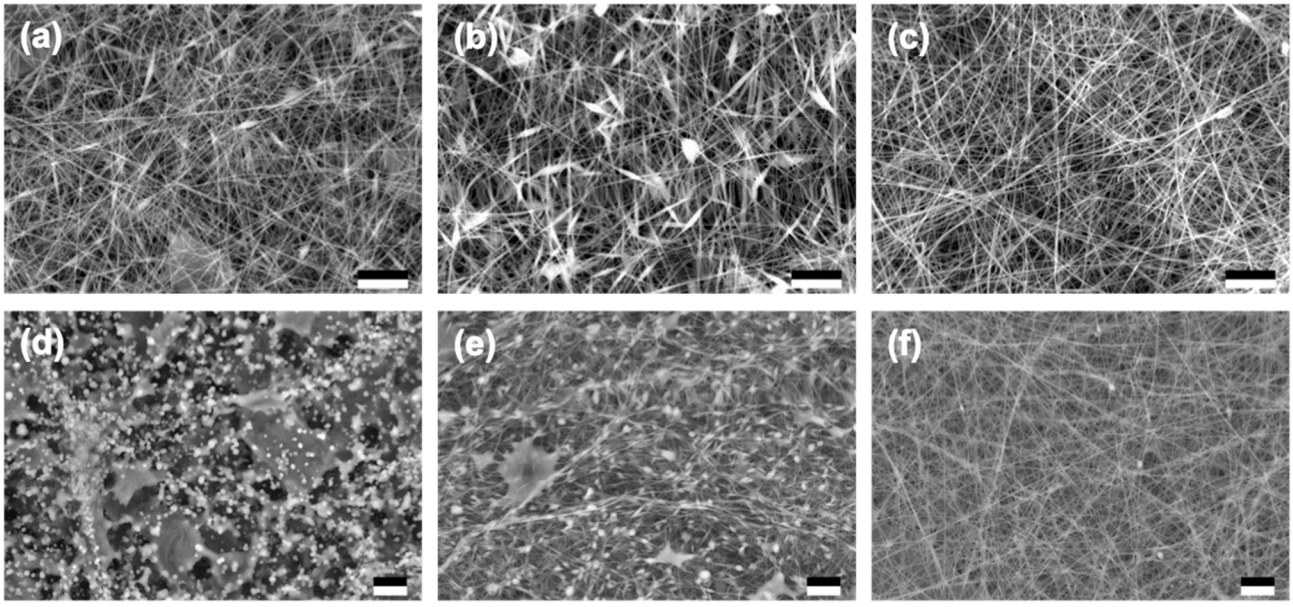

Figure 2. Scanning electron micrographs of blank PVA/PEO fibers electrospun at (a) 5 wt%, (b) 6 wt%, and (c) 7 wt% solution concentrations and MLT-loaded (5% w/w) PVA/PEO fibers electrospun at (d) 5 wt%, (e) 6 wt%, and (f) 7 wt% solution concentrations. Scale bar = 10 μm.

Average fiber diameters of 5%, 6%, and 7% PVA/PEO blend fibers are shown in Figure 3. The blank PVA/PEO fibers exhibited average fiber diameters in the range of 0.28 ± 0.05 μm and 0.33 ± 0.05 μm. The MLT-loaded fibers showed a slightly larger average fiber diameter for the 6% and 7% formulations (i.e., 0.29 ± 0.07 μm and 0.31 ± 0.07 μm, respectively) as compared to their counterparts. The 5% MLT-loaded PVA/PEO fibers displayed very minimal information of the fiber structure due to the reduced electrospinnability after incorporating MLT. Therefore, average fiber diameter data was excluded for the MLT-loaded 5% PVA/PEO fibers.

Electrospun pure PEO or PVA fibers have been reported elsewhere. Studies showed that electrospun PEO fibers exhibited fiber diameters from 0.36 to 1.06 μm at concentrations between 3 and 7 wt% [26]. Others reported the effects of molecular weight and polymer solution concentrations on the average fiber diameters of electrospun PEO fibers [27]. At a molecular weight of 1000 kDa, the average PEO fiber diameter increased from 206 ± 35 nm to 513 ± 75 nm as the polymer concentration increased from 3 to 6 wt%.

Similarly, effects of the solution properties and electrospinning conditions were investigated using PVA/kefiran solutions [28]. Results suggested that increasing polymer solution concentrations from 6 to 8%, fiber morphologies improved from beaded to uniform fibers with an average fiber diameter increased from 87 ± 14 to 246 ± 50 nm. Others also showed beading in lower concentrations of PVA solutions in electrospinning, while increasing degree of polymerization of the PVA decreased the average fiber diameter [29]. Incorporating additives had shown to improve PVA fiber morphologies with an increased average fiber diameter [30]. This finding suggested that additives in PVA solutions improved the electrospinnability of the PVA fibers. In general, our findings in electrospun fiber morphologies and average fiber diameters of blend PVA/PEO fibers were in agreement with the mentioned literature data from pure PVA and PEO fibers. Furthermore,

incorporating an additive (i.e., MLT) in PVA/PEO blend fiber system increased the average fiber diameter as compared to the blank counterparts.

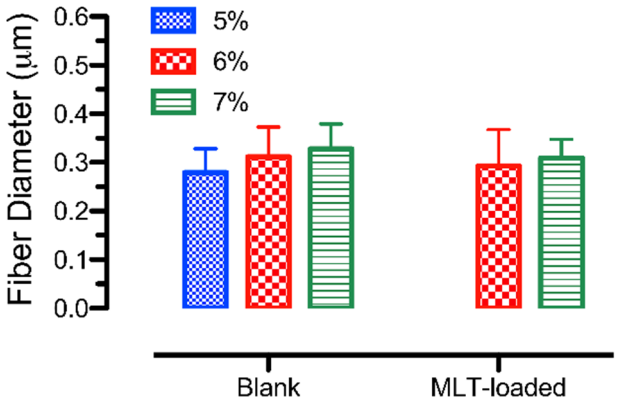

Figure 3. Average fiber diameters of blank and MLT-loaded PVA/PEO fibers electrospun at various polymer concentrations.

3.3. Mechanical properties

Uniaxial mechanical tests were conducted on dog-bone shaped PVA/PEO fiber meshes using a constant strain rate method. Stress-strain data was calculated from the raw load-displacement data. Representative stress-strain curves of the blank and MLT-loaded PVA/PEO fibers are shown in Figure 4. All samples exhibited an initial linear viscoelastic region, followed by a yield demonstrating the onset of permanent deformation of the molecular structures of the blend polymers [31]. After the yield, stress increased minimally with the continuous applied strain on the fiber samples (~ 100% strain). In this region, the stress-strain behavior was associated with the unfolding of the molecular chains of semicrystalline PVA and PEO [32]. The molecular chain unfolding process was terminated with the fracture of the molecular chain, and in a macro-scale, representing the fracture of the fibrous membranes. The stress-strain behaviors of the PVA/PEO fibers were in accordance with the reported literature [33].

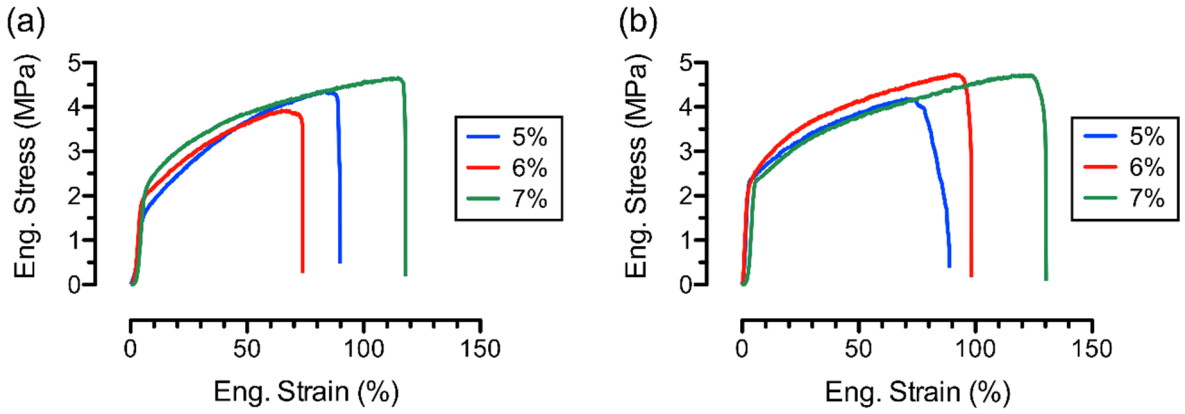

Figure 4. Representative stress-strain curves of (a) blank and (b) MLT-loaded PVA/PEO fibers electrospun at various polymer concentrations.

The average elastic moduli, shown in Figure 5(a), were 49.4 ± 9.5 MPa, 66.7 ± 6.4 MPa, and 86.8 ± 3.4 MPa for the 5%, 6%, and 7% blank PVA/PEO fibers, respectively. Increasing polymer concentration in the blend fibers produced a more well-defined non-woven fibrous structure, as shown in Figure 2, and hence, yielded a higher average elastic moduli [34]. Others reported a decrease in average elastic moduli using the single fiber test method as the average fiber diameter increased from several hundreds of nanometer to a few micrometers due to the increases in polymer concentration in electrospinning, suggesting the effects of microscopic defects in fibers on the mechanical properties [35]. Similarly, the average elastic moduli were 100.9 ± 6.5 MPa, 121.1 ± 6.9 MPa, and 143.6 ± 3.1 MPa for the 5%, 6%, and 7% MLT-loaded PVA/PEO fibers, respectively. The MLT-loaded PVA/PEO fibers exhibited significantly higher elastic moduli than the blank fibers ($P < 0.05$). This finding suggested the role of MLT as an excipient in the fiber structure that provided the additional stiffening mechanism in the fiber mesh [36].

The average tensile strength of the blank PVA/PEO fibers, shown in Figure 5(b), decreased from 4.5 ± 0.4 to 3.8 ± 0.1 MPa as the polymer concentration increased from 5 to 7%. Similar trends were found on the average tensile strength of the MLT-loaded PVA/PEO fibers as the average tensile strength decreased from 5.1 ± 0.4 to 4.5 ± 0.3 MPa when the polymer concentration increased from 5 to 7%. The decrease in average tensile strength was related to macroscopic defects, including nonwoven fiber-fiber sliding interactions, fiber orientations, and fiber diameters [37]. More importantly, the MLT-loaded PVA/PEO fibers exhibited a higher tensile strength than the blank counterparts, similar to the effects in average elastic moduli.

The average elongation to failure of the blank and MLT-loaded PVA/PEO fibers, shown in Figure 5(c), increased as the polymer concentration increased. Both blank and MLT-loaded PVA/PEO fibers exhibited an average elongation to failure in the range of 100 to 119% with the MLT-loaded fibers having a larger average elongation to failure than the blank counterparts.

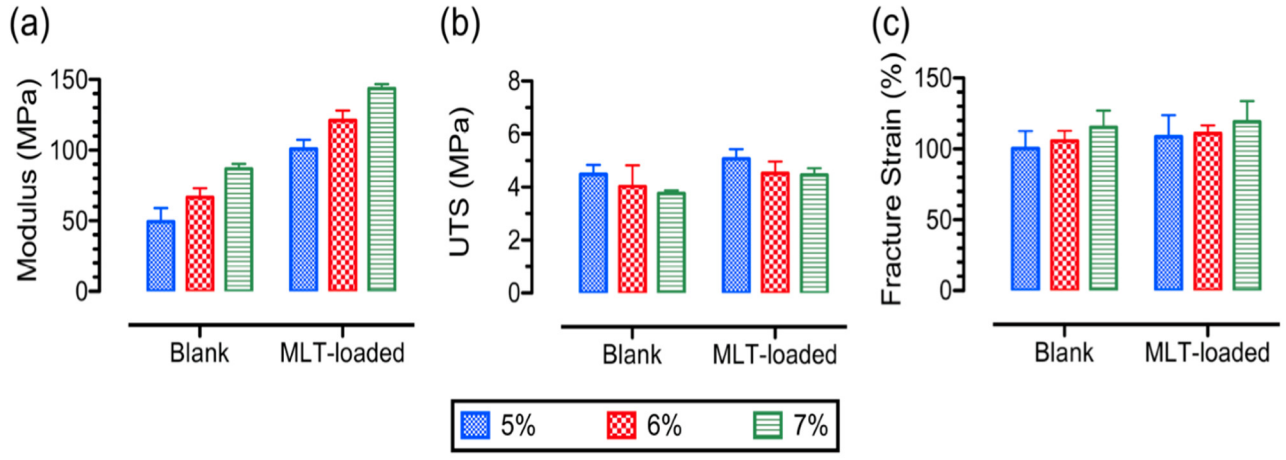

Figure 5. Mechanical properties of blank and MLT-loaded PVA/PEO electrospun fibers, showing (a) average elastic moduli, (b) average ultimate tensile strength (UTS), and (c) average fracture strain at various polymer concentrations.

3.4. In vitro dissolution studies

Both PVA and PEO are water-soluble polymers and are widely used as a fast-dissolving polymer matrix for drug carriers in oral drug delivery. To evaluate the dissolution properties of the blend PVA/PEO fibers, we placed a 4-μL droplet on top of each fiber disc to measure the opening of the dissolved fiber area for indications of the mass loss. Figure 6(a) shows the average percentage of mass losses for the blank and MLT-loaded PVA/PEO fibers at various polymer concentrations. According to the results, a general decreasing trend in the average percentage of mass loss was obtained in both blank and MLT-loaded PVA/PEO fibers when increasing the polymer concentrations. Studies showed that dissolution of semicrystalline polymer fibers involved in the process of solvent penetration, crystallite transformation into amorphous domains, domain/matrix swelling, followed by chain disentanglement (rate-limiting step) [38]. Similar to a study that the PVA/PEO fibers dissolved instantaneously (e.g., < 1s) [39], the 4-μL droplet method used in our work showed an average polymer dissolution of 1 ~ 1.5 wt%, resulting in an average percentage mass losses in between 4.6 ± 1.5% and 6.6 ± 0.3% for blank and MLT-loaded PVA/PEO fibers. In addition, incorporation of the MLT in the PVA/PEO fibers appeared to have minimal effects on the average percentage of mass loss, perhaps due to the marginal water solubility of the MLT [40].

Surface wettability of the electrospun fibrous membranes has an implication on the initial wetting of the fiber surfaces, which later triggers drug dissolution at the fiber surfaces and drug diffusion from the fiber core. Figure 6(b) shows the average water contact angle for the blank and MLT-loaded PVA/PEO fibers at various polymer concentrations. Increasing polymer concentration slightly increased the average water contact angles for both the blank and MLT-loaded PVA/PEO fibers. All fiber formulation exhibited an average water contact angle below 90°, indicating a hydrophilic surface property. Our findings were in agreement with the literature reported values [41]. Furthermore, incorporation of the MLT in the PVA/PEO fibers appeared to slightly decrease the average water contact angle within each fiber group, suggesting the role of hydrophilic MLT on the promotion of the surface wettability of the fibers.

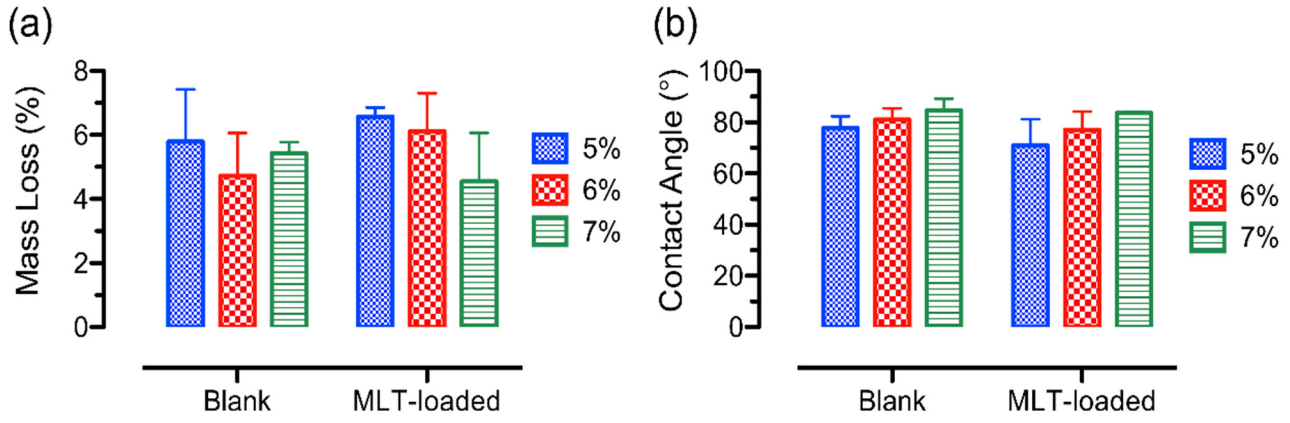

Figure 6. In vitro dissolution studies for blank and MLT-loaded PVA/PEO electrospun fiber mats, showing (a) average mass losses from 4-μL droplet studies and (b) average contact angles at various polymer concentrations.

3.5. In vitro drug release assays

In vitro drug release assays were performed using sink condition at 37 °C. Prior to measuring the MLT concentrations of the unknown samples as results of drug release from the PVA/PEO fibers, a MLT standard curve was established in Figure 7(a). A linear correlation of the absorption intensities at various MLT concentrations, ranging from 400 to 25 μg/mL, was obtained with a R-square value of 0.98. The equation of the linear curve was used to determine MLT concentrations of the unknown samples from each time-point to determine the cumulative release curves of MLT.

The in vitro MLT release profiles from various concentrations of PVA/PEO fibers are shown in Figure 7(b). As seen from the figure, the 5% PVA/PEO fibers exhibited a steeper initial slope as compared to the 6% and 7% PVE/PEO fibers, demonstrating the fast release behavior within 10 minutes. The initial burst release behavior of MLT decreased as the PVA/PEO concentrations increased in the electrospun fibers potentially due to increasing amount of the polymer matrix for the encapsulation of MLT. This finding was in agreement with the reported literature results on the in vitro release of rifampin from electrospun polylactic acid fibers at various concentrations [42]. Specifically, the 5% PVA/PEO reached 50% cumulative MLT release at around 3 minutes, whereas the 6% and 7% PVA/PEO fibers required more than 6 minutes to achieve 50% MLT release. Using one-phase association approach for the non-linear curve fit, the rate constants (K) were 0.203, 0.070, and 0.063 for the 5%, 6%, and 7% PVA/PEO fibers, respectively. The 5% PVA/PEO fibers yielded a total release of MLT of 82.9 ± 2.8% at 10 minutes, whereas the 6% and 7% PVA/PEO fibers exhibited 69.0 ± 2.4% and 60.9 ± 3.8% MLT release at 10 minutes, respectively. Our results showed that the 7% PVA/PEO fibers provided the most steady release rate from the sink assay, which was the closest to the desirable zero-order release, similar to the reported MLT release profile using cotton fiber as the carrier [43].

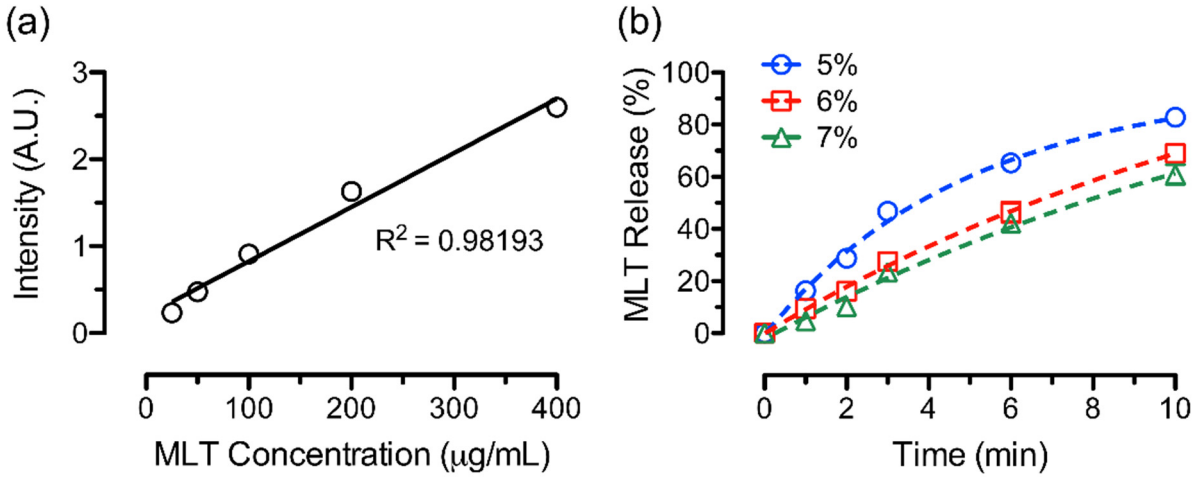

Figure 7. In vitro MLT release assays, showing (a) the standard curve of the MLT and (b) the release profiles of MLT from PVA/PEO fibers electrospun at various polymer concentrations.

In a study, PVA fibers were electrospun to encapsulate an antibacterial agent, chlorhexidine (CHX), at 2 wt% loading [44]. The pristine/untreated CHX-loaded PVA fibers showed a single step of 100% burst release in a few minutes. Others electrospun PVA fibers to incorporate sildenafil citrate (SC), up to 5 wt% loading, and the in vitro release data demonstrated burst release profiles in 4 minutes (i.e., ~100% release) [45]. Similar to PVA, PEO is a water-soluble polymer and has been widely used in electrospun fibers to improve the surface wettability of the hydrophobic fibers for modulations of the in vitro drug release rates [46,47]. In contrast to the PVA and PEO fibers for fast drug delivery systems, most of the reported works in fast-dissolving fibers for oral drug delivery consisted of polyvinylpyrrolidone (PVP) matrix [48,49]. However, drug-loaded PVP fibers were often electrospun using an organic solvent (e.g., alcohol-based solvents, dimethylformamide, chloroform, etc.), which raised the concerns of degrading bioactivities of the drugs and increasing cytotoxicity on mucosal tissues due to the residual solvent in the fibers. In general, our in vitro drug release studies demonstrated the ability to achieve fast MLT release rate (i.e., within 10 minutes) with a zero-ordered release profile using blend PVA/PEO fibers and DI-water as the solvent for electrospinning.

3.6. In vitro cell viability assays

The viabilities of HUVECs were evaluated by MTT assays in the presence of blank and MLT-loaded PVA/PEO fibers, and the results are shown in Figure 8. The UV absorption of formazan forming crystals, indicating mitochondrial function of the living cells, suggested a minimal cytotoxicity level at 24 hours of treatment with both blank and MLT-loaded fibers as compared to the control groups. Consequently, the electrospun PVA/PEO fibers and those with the incorporation of MLT were compatible with HUVECs within 24 hours. Similar studies have shown compatibility of electrospun PVA and/or PEO fibers with various cells [50–52]. In addition, studies showed that MLT down-regulated pro-inflammatory cytokines (e.g., IL-1β and IL-6) as well as anti-inflammatory cytokine (e.g., TNFα) and promoted angiogenesis [53]. More importantly, MLT showed dose-dependent inhibition of the viability of HUVECs, where the viability and angiogenesis suppression of HUVECs were associated with down-regulating of the hypoxia/HIF-1α/ROS/VEGF pathway [54]. In general, our findings showed that both blank and MLT-loaded PVA/PEO fibers were compatible with HUVECs in vitro at 24 hours.

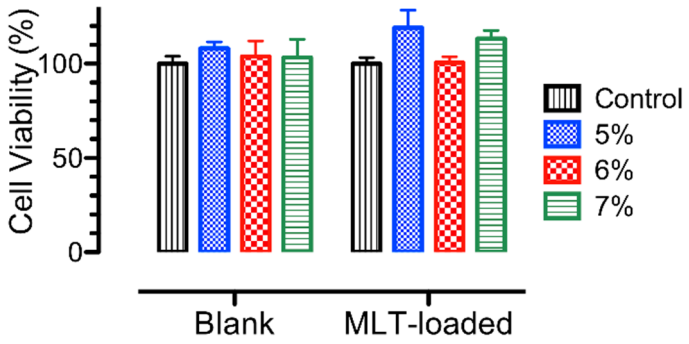

Figure 8. In vitro HUVEC viability studies at 24 hours using blank and MLT-loaded PVA/PEO fibers electrospun at various polymer concentrations.

4. Conclusions

In conclusion, our study showed that electrospun MLT-loaded blend PVA/PEO (50/50) fibers at various polymer compositions (e.g., 5%, 6%, and 7%) exhibited time-dependent release characteristics within 10 minutes, suitable for fast drug delivery applications. The time dependent release characteristics were associated with the dissolution rates of the PVA/PEO fiber mats. Improving electrospinnability of the PVA/PEO solutions facilitated the fiber mat structure, where our study showed correlations between electrospun fiber morphologies and average diameters with the viscosities of the PVA/PEO solutions. All MLT-loaded PVA/PEO blend fibers exhibited excellent compatibilities with HUVECs over 24 hours, suggesting the potential use of electrospun blend PVA/PEO fibers for topical and/or mucoadhesive drug delivery.

Acknowledgements

The authors thank the Department of Mechanical Engineering, College of Engineering, at the University of Texas at Tyler for supporting the investigation of blend PVA/PEO fibers for oral drug delivery.

Conflict of interest

The authors declare that they have no known competing financial interests or personal relationships that could have appeared to influence the work reported in this paper.

References

1. Szunerits S and Boukherroub R (2018) Heat: A highly efficient skin enhancer for transdermal drug delivery. *Front Bioeng Biotechnol* 6: 15. https://doi.org/10.3389/fbioe.2018.00015
2. Alshehri S, Imam SS, Hussain A, et al. (2020) Potential of solid dispersions to enhance solubility, bioavailability, and therapeutic efficacy of poorly water-soluble drugs: newer formulation techniques, current marketed scenario and patents. *Drug Deliv* 27: 1625–1643. https://doi.org/10.1080/10717544.2020.1846638
3. Prajapati SK, Jain A, Jain A, et al. (2019) Biodegradable polymers and constructs: A novel approach in drug delivery. *Eur Polym J* 120: 109191. https://doi.org/10.1016/j.eurpolymj.2019.08.018
4. Waly AL, Abdelghany AM, Tarabiah AE (2021) Study the structure of selenium modified polyethylene oxide/polyvinyl alcohol (PEO/PVA) polymer blend. *J Mater Res Technol* 14: 2962–2969. https://doi.org/10.1016/j.jmrt.2021.08.078
5. Bala R, Khanna S, Pawar P (2014) Design optimization and *in vitro* - *in vivo* evaluation of orally dissolving strips of clobazam. *J Drug Deliv* 2014: 1–15. https://doi.org/10.1155/2014/392783
6. Yun YH, Lee BK, Park K (2015) Controlled drug delivery: Historical perspective for the next generation. *J Controlled Release* 219: 2–7. https://doi.org/10.1016/j.jconrel.2015.10.005
7. Chou S-F, Carson D, Woodrow KA (2015) Current strategies for sustaining drug release from electrospun nanofibers. *J Controlled Release* 220: 584–591. https://doi.org/10.1016/j.jconrel.2015.09.008

8. Gizaw M, Thompson J, Faglie A, et al. (2018) Electrospun fibers as a dressing material for drug and biological agent delivery in wound healing applications. *Bioengineering* 5: 9. https://doi.org/10.3390/bioengineering5010009
9. Chou S-F and Woodrow KA (2017) Relationships between mechanical properties and drug release from electrospun fibers of PCL and PLGA blends. *J Mech Behav Biomed Mater* 65: 724–733. https://doi.org/10.1016/j.jmbbm.2016.09.004
10. Ball C, Chou S-F, Jiang Y, et al. (2016) Coaxially electrospun fiber-based microbicides facilitate broadly tunable release of maraviroc. *Mater Sci Eng C* 63: 117–124. https://doi.org/10.1016/j.msec.2016.02.018
11. Bagheri M, Validi M, Gholipour A, et al. (2022) Chitosan nanofiber biocomposites for potential wound healing applications: Antioxidant activity with synergic antibacterial effect. *Bioeng Transl Med* 7: e10254. https://doi.org/10.1002/btm2.10254
12. Moroni I and Garcia-Bennett AE (2021) Effects of absorption kinetics on the catabolism of melatonin released from CAP-coated mesoporous silica drug delivery vehicles. *Pharmaceutics* 13: 1436. https://doi.org/10.3390/pharmaceutics13091436
13. Al-Zaqri N, Pooventhiran T, Alsalme A, et al. (2020) Structural and physico-chemical evaluation of melatonin and its solution-state excited properties, with emphasis on its binding with novel coronavirus proteins. *J Mol Liq* 318: 114082. https://doi.org/10.1016/j.molliq.2020.114082
14. Hawkins BC, Burnett E, Chou S-F (2022) Physicomechanical properties and in vitro release behaviors of electrospun ibuprofen-loaded blend PEO/EC fibers. *Mater Today Commun* 30: 103205. https://doi.org/10.1016/j.mtcomm.2022.103205
15. ASTM D1708-18 (2018) Standard test method for tensile properties of plastics by use of microtensile specimens, West Conshohocken, PA, ASTM International
16. ASTM D5034-21 (2021) Standard test method for breaking strength and elongation of textile fabrics (grab test), West Conshohocken, PA, ASTM International.
17. Hekmati AH, Khenoussi N, Nouali H, et al. (2014) Effect of nanofiber diameter on water absorption properties and pore size of polyamide-6 electrospun nanoweb. *Text Res J* 84: 2045–2055. https://doi.org/10.1177/0040517514532160
18. Daescu M, Toulbe N, Baibarac M, et al. (2020) Photoluminescence as a complementary tool for UV-VIS spectroscopy to highlight the photodegradation of drugs: A case study on melatonin. *Molecules* 25: 3820. https://doi.org/10.3390/molecules25173820
19. Haro Durand L, Vargas G, Vera-Mesones R, et al. (2017) In vitro human umbilical vein endothelial cells response to ionic dissolution products from lithium-containing 45S5 bioactive glass. *Materials* 10: 740. https://doi.org/10.3390/ma10070740
20. Amariei N, Manea LR, Bertea AP, et al. (2017) The influence of polymer solution on the properties of electrospun 3D nanostructures. *IOP Conf Ser Mater Sci Eng* 209: 012092. https://doi.org/10.1088/1757-899X/209/1/012092
21. Datta R, Yelash L, Schmid F, et al. (2021) Shear-thinning in oligomer melts—Molecular origins and applications. *Polymers* 13: 2806. https://doi.org/10.3390/polym13162806
22. Mirtič J, Balažic H, Zupančič Š, et al. (2019) Effect of solution composition variables on electrospun alginate nanofibers: Response surface analysis. *Polymers* 11: 692. https://doi.org/10.3390/polym11040692

23. Briscoe B, Luckham P, Zhu S (2000) The effects of hydrogen bonding upon the viscosity of aqueous poly(vinyl alcohol) solutions. *Polymer* 41: 3851–3860. https://doi.org/10.1016/S0032-3861(99)00550-9
24. Vlachou M, Siamidi A, Anagnostopoulou D, et al. (2022) Modified release of the pineal hormone melatonin from matrix tablets containing poly(*L*-lactic acid) and its PLA-*co*-PEAd and PLA-*co*-PBAd copolymers. *Polymers* 14: 1504. https://doi.org/10.3390/polym14081504
25. Angel N, Li S, Yan F, et al. (2022) Recent advances in electrospinning of nanofibers from bio-based carbohydrate polymers and their applications. *Trends Food Sci Technol* 120: 308–324. https://doi.org/10.1016/j.tifs.2022.01.003
26. Son WK, Youk JH, Lee TS, et al. (2004) The effects of solution properties and polyelectrolyte on electrospinning of ultrafine poly(ethylene oxide) fibers. *Polymer* 45: 2959–2966. https://doi.org/10.1016/j.polymer.2004.03.006
27. Filip P and Peer P (2019) Characterization of poly(ethylene oxide) nanofibers—Mutual relations between mean diameter of electrospun nanofibers and solution characteristics. *Processes* 7: 948. https://doi.org/10.3390/pr7120948
28. Ziyadi H, Baghali M, Bagherianfar M, et al. (2021) An investigation of factors affecting the electrospinning of poly (vinyl alcohol)/kefiran composite nanofibers. *Adv Compos Hybrid Mater* 4: 768–779. https://doi.org/10.1007/s42114-021-00230-3
29. Mwiiri FK and Daniels R (2020) Influence of PVA molecular weight and concentration on electrospinnability of birch bark extract-loaded nanofibrous scaffolds intended for enhanced wound healing. *Molecules* 25: 4799. https://doi.org/10.3390/molecules25204799
30. Cho D, Netravali AN, Joo YL (2012) Mechanical properties and biodegradability of electrospun soy protein isolate/PVA hybrid nanofibers. *Polym Degrad Stab* 97: 747–754. https://doi.org/10.1016/j.polymdegradstab.2012.02.007
31. Amjadi M and Fatemi A (2020) Tensile behavior of high-density polyethylene including the effects of processing technique, thickness, temperature, and strain rate. *Polymers* 12: 1857. https://doi.org/10.3390/polym12091857
32. Séguéla R (2007) Plasticity of semi-crystalline polymers: crystal slip versus melting-recrystallization. *E-Polym* 7: 32. https://doi.org/10.1515/epoly.2007.7.1.382
33. Devangamath SS, Lobo B, Masti SP, et al. (2020) Thermal, mechanical, and AC electrical studies of PVA–PEG–Ag2S polymer hybrid material. *J Mater Sci Mater Electron* 31: 2904–2917. https://doi.org/10.1007/s10854-019-02835-3
34. Rashid TU, Gorga RE, Krause WE (2021) Mechanical properties of electrospun fibers—A critical review. *Adv Eng Mater* 23: 2100153. https://doi.org/10.1002/adem.202100153
35. Morel A, Domaschke S, Urundolil Kumaran V, et al. (2018) Correlating diameter, mechanical and structural properties of poly(L-lactide) fibres from needleless electrospinning. *Acta Biomater* 81: 169–183. https://doi.org/10.1016/j.actbio.2018.09.055
36. Parab RS and Rao GK (2019) Understanding the mechanical properties of polymer blends in the presence of plasticizers and other additives. *Int J Pharm Sci Rev Res* 54: 84–91.
37. Croisier F, Duwez A-S, Jérôme C, et al. (2012) Mechanical testing of electrospun PCL fibers. *Acta Biomater* 8: 218–224. https://doi.org/10.1016/j.actbio.2011.08.015
38. Ghasemi M, Singapati AY, Tsianou M, et al. (2017) Dissolution of semicrystalline polymer fibers: Numerical modeling and parametric analysis. *AIChE J* 63: 1368–1383. https://doi.org/10.1002/aic.15615

39. Hirsch E, Pantea E, Vass P, et al. (2021) Probiotic bacteria stabilized in orally dissolving nanofibers prepared by high-speed electrospinning. *Food Bioprod Process* 128: 84–94. https://doi.org/10.1016/j.fbp.2021.04.016
40. Zhang J, Yan X, Tian Y, et al. (2020) Synthesis of a new water-soluble melatonin derivative with low toxicity and a strong effect on sleep aid. *ACS Omega* 5: 6494–6499. https://doi.org/10.1021/acsomega.9b04120
41. Khan MQ, Kharaghani D, Nishat N, et al. (2019) Preparation and characterizations of multifunctional PVA/ZnO nanofibers composite membranes for surgical gown application. *J Mater Res Technol* 8: 1328–1334. https://doi.org/10.1016/j.jmrt.2018.08.013
42. Song X, Gao Z, Ling F, et al. (2012) Controlled release of drug via tuning electrospun polymer carrier. *J Polym Sci Part B Polym Phys* 50: 221–227. https://doi.org/10.1002/polb.23005
43. Mihailiasa M, Caldera F, Li J, et al. (2016) Preparation of functionalized cotton fabrics by means of melatonin loaded β-cyclodextrin nanosponges. *Carbohydr Polym* 142: 24–30. https://doi.org/10.1016/j.carbpol.2016.01.024
44. Gulino EF, Citarrella MC, Maio A, et al. (2022) An innovative route to prepare in situ graded crosslinked PVA graphene electrospun mats for drug release. *Compos Part Appl Sci Manuf* 155: 106827. https://doi.org/10.1016/j.compositesa.2022.106827
45. Torres-Martínez EJ, Vera-Graziano R, Cervantes-Uc JM, et al. (2020) Preparation and characterization of electrospun fibrous scaffolds of either PVA or PVP for fast release of sildenafil citrate. *E-Polym* 20: 746–758. https://doi.org/10.1515/epoly-2020-0070
46. Carvalho LD de, Peres BU, Maezono H, et al. (2019) Doxycycline release and antibacterial activity from PMMA/PEO electrospun fiber mats. *J Appl Oral Sci* 27: e20180663. https://doi.org/10.1590/1678-7757-2018-0663
47. Eskitoros-Togay ŞM, Bulbul YE, Tort S, et al. (2019) Fabrication of doxycycline-loaded electrospun PCL/PEO membranes for a potential drug delivery system. *Int J Pharm* 565: 83–94. https://doi.org/10.1016/j.ijpharm.2019.04.073
48. Yu D-G, Shen X-X, Branford-White C, et al. (2009) Oral fast-dissolving drug delivery membranes prepared from electrospun polyvinylpyrrolidone ultrafine fibers. *Nanotechnology* 20: 055104. https://doi.org/10.1088/0957-4484/20/5/055104
49. Samprasit W, Akkaramongkolporn P, Ngawhirunpat T, et al. (2015) Fast releasing oral electrospun PVP/CD nanofiber mats of taste-masked meloxicam. *Int J Pharm* 487: 213–222. https://doi.org/10.1016/j.ijpharm.2015.04.044
50. Huang C-Y, Hu K-H, Wei Z-H (2016) Comparison of cell behavior on pva/pva-gelatin electrospun nanofibers with random and aligned configuration. *Sci Rep* 6: 37960. https://doi.org/10.1038/srep37960
51. Yang JM, Yang JH, Tsou SC, et al. (2016) Cell proliferation on PVA/sodium alginate and PVA/poly(γ-glutamic acid) electrospun fiber. *Mater Sci Eng C* 66: 170–177. https://doi.org/10.1016/j.msec.2016.04.068
52. Carrasco-Torres G, Valdés-Madrigal M, Vásquez-Garzón V, et al. (2019) Effect of silk fibroin on cell viability in electrospun scaffolds of polyethylene oxide. *Polymers* 11: 451. https://doi.org/10.3390/polym11030451
53. Cerqueira A, Romero-Gavilán F, Araújo-Gomes N, et al. (2020) A possible use of melatonin in the dental field: Protein adsorption and in vitro cell response on coated titanium. *Mater Sci Eng C* 116: 111262. https://doi.org/10.1016/j.msec.2020.111262

54. Cheng J, Yang H, Gu C, et al. (2018) Melatonin restricts the viability and angiogenesis of vascular endothelial cells by suppressing HIF-1α/ROS/VEGF. *Int J Mol Med* 43: 945–955. https://doi.org/10.3892/ijmm.2018.4021